agronomy

MDPI

Article

Dynamic Carbohydrate Supply and Demand Model of Vegetative Growth: Response to Temperature, Light, Carbon Dioxide, and Day Length

Martin P.N. Gent *

Forestry and Horticulture, Connecticut Agricultural Experiment Station, New Haven, CT 06504-1106, USA; Martin.Gent@ct.gov

Received: 29 November 2017; Accepted: 13 February 2018; Published: 16 February 2018

Abstract: Predicting the growth response of seedlings from the environmental responses of photosynthesis and metabolism may be improved by considering the dynamics of non-structural carbohydrate (NSC) over a diurnal cycle. Attenuation of growth metabolism when NSC content is low could explain why some NSC is conserved through the night. A dynamic model, incorporating diurnal variation in NSC, is developed to simulate growth of seedlings hour-by-hour. I compare predictions of this model to published growth and NSC data for seedlings that varied according to temperature, light, day length, or CO_2. Prolonged-darkness experiments show a temperature dependent upper limit on the respiration capacity. Respiration is attenuated as NSC is depleted. Furthermore, when NSC is high at dawn, inhibition of photosynthesis could attenuate the accumulation of NSC under low temperature, high light, or high CO_2. These concepts are used to simulate plant metabolism and growth rates and diurnal variation of NSC in tomato seedlings under two light levels and various temperatures. Comparison of other results using the same model parameters show the dynamic model could predict results for starch and starch-less plants, and when growth was affected by CO_2 enrichment and day length.

Keywords: carbohydrate starvation; non-structural carbohydrate; photosynthesis; photosynthesis inhibition; respiration; relative growth rate; structure; diurnal variation

1. Introduction

1.1. Supply and Demand

Photosynthesis is the limiting factor in most crop growth models [1–4], but metabolism may also limit growth. If one assumes that low temperature limits growth, relative to the optimum for a species of plant, then the temperature dependence of metabolism may become a limiting factor under increasing CO_2 levels. In the range from 10 to 25 °C, the demand for carbohydrate increases exponentially with temperature. The growth response of lettuce (*Lactuca sativa*) has a Q_{10} = 3.3 [5], and the extension of wheat leaves (*Triticum aestivum*) has a Q_{10} that varies from 2.5 to 3.5 [6]. Growth appears to be limited at warm temperatures for two reasons: a decrease in photosynthesis and an increase in respiration. The temperature response of photosynthesis is concave, first increasing and then decreasing with increasing temperature [7]. In the model of Farquhar, van Caemmerer, and Berry [8], the loss of photosynthesis at temperatures above 40 °C is due to a continuous decrease in the ratio of CO_2 to O_2 binding, as well as a breakdown in the conversion of light to chemical energy.

Recently, Gent and Seginer [9] developed a steady state model based on the hypothesis that growth is the minimum of the supply of non-structural carbohydrate, NSC, from photosynthesis, and the demand of NSC to synthesize new tissue. NSC includes soluble sugar, starch, and fructans. This model predicted the effects of temperature and light on vegetative plants growing in a constant

environment. The model also simulated acclimation to temperature as a transient process under these conditions. It provided a plausible interpretation of demand- and supply-limited growth data, and could be used to demonstrate the difference between short-term effects of temperature as a transient process, and long-term effects resulting in acclimation [10].

1.2. Carbon Starvation

The NSC from photosynthesis during daylight hours is not fully consumed by biosynthesis in the dark, because some NSC is observed at dawn even under warm temperatures, where demand should exceed supply. This amount was defined as a required reserve in the steady-state model [9]. Experiments done under prolonged darkness show a decrease of respiration and NSC with time, and higher respiration due to higher NSC for plants grown under higher light before darkness [11]. Carbohydrate reserves were depleted within 48-h in *Pennisetum glaucum* [12] and *Zea mays* [13], while loss of proteins was much slower. Respiration followed a decreasing pattern over several days in tomato (*Solanum lycopersicon*) [14], and sugars were depleted within one day in excised tomato roots, while starch and proteins fell more slowly [15]. As NSC decreased over two weeks, dark respiration and leaf elongation rate fell in *Festuca arundinacea* [16]. A similar response was seen in *Medicago sativa* [17]. These authors considered respiration as the sum of maintenance respiration represented by an intercept (about 30% of maximum), and growth respiration proportional to NSC. I propose that the consumption of NSC continues in the dark, at a rate which decreases as NSC is consumed, and that this governs the growth.

1.3. Photosynthesis Inhibition

Evidence suggests that high NSC tends to inhibit photosynthesis. The NSC still available at dawn was negatively correlated with growth [18]. Net photosynthesis of Beet (*Beta vulgaris*) was reduced by 15% as starch plus sugar content increased over a day [19]. Even when spinach (*Spinacea oleracea*) showed no intra-day variation of photosynthesis, a significant inhibition was observed as NSC accumulated from one day to the next [20]. The NSC in tomato leaves was considerably higher in spring than in winter [21], and this was correlated with more inhibition of photosynthesis around noon time in the spring. I claim sink inhibition is required to model growth and NSC metabolism in plants. There was feedback inhibition of NSC on photosynthesis in the steady-state model [9]. It is not clear whether this inhibition changes within the photoperiod or only from one day to the next.

1.4. Starch-Less Mutants

In starch-synthesizing plants, part of the NSC retained in the leaf as starch is remobilized to export sucrose to other parts of the plant in the dark [22–24]. Two sets of observations show that starch turnover is highly regulated. First, only a small amount of starch is left in plants at the end of the night [19,25,26]. This implies that the rate of starch accumulation in the light is coordinated with the rate of utilization during the dark. This balance could be due to regulated export rather than photosynthesis, resulting in more export when there is more NSC. Second, to provide carbon to support metabolism and export during a long night, a larger proportion of the photo-assimilate is partitioned to starch in short- compared to long-day conditions [25,27]. Do these mechanisms contribute to the stimulation of starch synthesis in short days when less carbon is available? The sugars that accumulate in leaves during the day are depleted by rapid respiration in the first part of the night to reduce growth in starch-less mutants of Arabidopsis (*Arabidopsis thaliana)* [28,29]. I wish to know if starch-less mutants regulate NSC metabolism to assure some NSC is available for growth and respiration during the night.

1.5. Seedlings Compared to Larger Plants

Seedlings tend to grow exponentially, as least for a few weeks, with all parts increasing in a similar fashion. The relative growth rate of seedlings can be related to the environment. There is no indication how much of the leaf, stem, and root biomass is involved in growth of larger plants. To

analyze growth for larger plants and for longer growing times than used here, the relationships between photosynthesis, respiration, and plant growth must be determined separately for each plant species.

1.6. Objectives

I develop a dynamic model to explain the variation in NSC over the diurnal cycle, based on hourly rates of metabolism and response to NSC. This model does not include a correction for nitrogen or any other nutrient. Such a model predicts the rate of NSC metabolism in seedlings, along with maximum and minimum NSC over the day, in response to various environmental conditions, such as light, temperature, CO_2 concentration, and day length. It may predict relative growth rates better than the steady-state model [9]. I incorporate sink inhibition of photosynthesis in the model, and assume that starch synthesis and breakdown provide sufficient NSC for growth and respiration during both day and night.

2. Model Development

The model has two state variables: structural dry matter, $\mathbf{S}$, in g[SDM] m^{-2}[ground] and non-structural dry matter, $\mathbf{C}$ in g[CHO] m^{-2}[ground] [10]. Figure 1 is a summary flow diagram showing the state variables, rate variables, and driving variables (light, temperature, CO_2) of the model. The terms "carbohydrate" (CHO) and "non-structural carbohydrate" (NSC) are considered synonyms, and dry matter (DM) stands for the combined nonstructural, and structural dry matter.

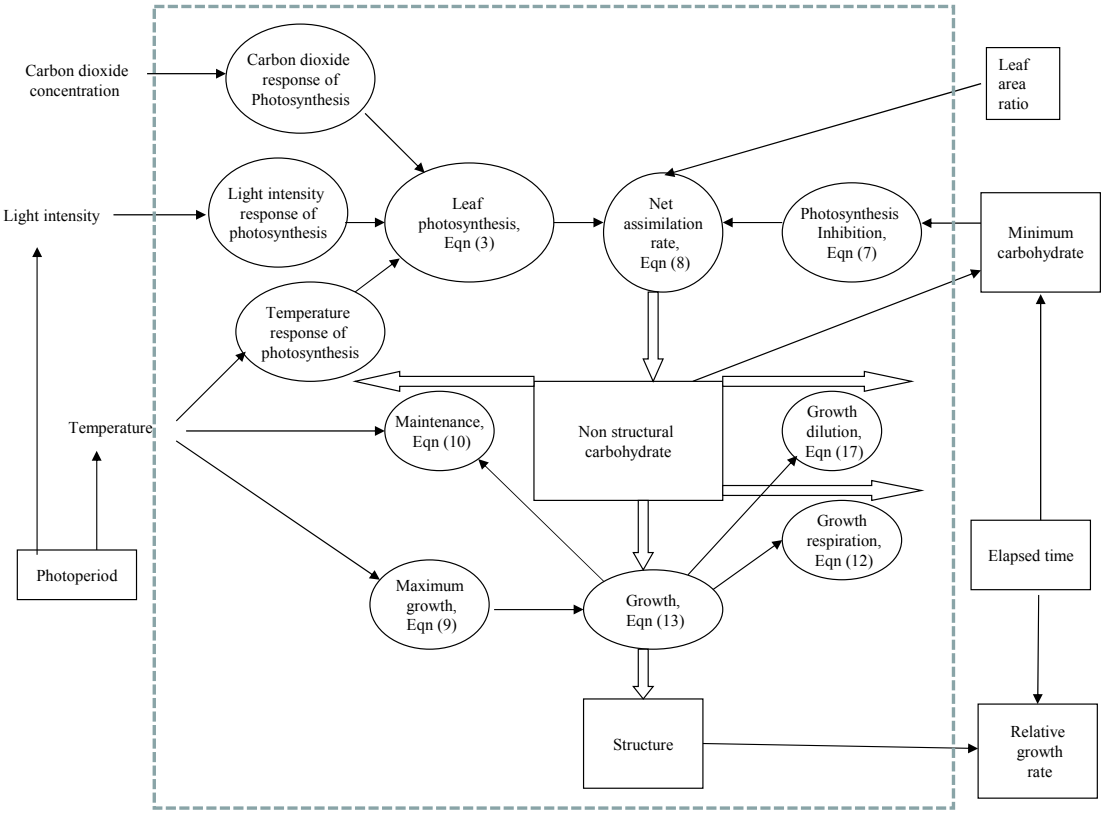

Figure 1. Schematic diagram of the hourly calculations of the dynamic model. Rectangles indicate state variables. Those outside the calculation are daily variables. Ellipses indicate rate equations. Text values are driving variables. The flow of NSC is indicates by thick arrows. Influences on rate equations are indicated by thin arrows.

The differential rate equations are

$$\frac{\mathrm{d}\mathbf{S}}{\mathrm{d}t} = \mathbf{s} \tag{1}$$

and

$$\frac{\mathrm{d}\mathbf{C}}{\mathrm{d}t} \equiv \mathbf{c} = \mathbf{p} - \mathbf{i} - \mathbf{m} - \mathbf{g} - \mathbf{s} - C \bullet s \tag{2}$$

where $\mathbf{s}$ is structural growth rate and $\mathbf{c}$ is the rate of change of $\mathbf{C}$. Furthermore, $\mathbf{p}$ is potential gross photosynthesis rate, $\mathbf{i}$ is inhibited photosynthesis, $\mathbf{m}$ is maintenance respiration, and $\mathbf{g}$ is growth respiration, all in g[DM] m^{-2}[ground] h^{-1}. The parameters mentioned here, and used later in the model, are defined in the Abbreviations, normalized per gram [SDM].

Photosynthesis is the only process that increases **C**. I assume that potential photosynthesis per unit lit leaf area, p, is a product of three functions, one of light, L (in μmol[PAR] m^{-2}[leaf] s^{-1}), one of temperature, T (in °C), and one of carbon dioxide concentration, C_a (in μmol[CO_2] mol^{-1}[air]):

$$p\{L,T,C_a\} = P_{\max} f\{L\} h\{T\} k\{C_a\} = P_{\max}\left[\frac{L}{\gamma + L}\right]\left[1 - \kappa(T - \tau)^2\right]\left[\frac{C_a}{\delta + C_a}\right] \tag{3}$$

where P_{max}, in g[DM] m^{-2}[leaf] h^{-1}, is maximum photosynthetic rate and f, h and k are dimensionless correction terms, all positive and smaller than one. This is similar to the version of Gent and Seginer [9], with an extra term for CO_2. It fits the data of single leaf photosynthesis of tomato under various conditions of light, temperature and CO_2 (data not shown). Photosynthesis on a leaf area basis expressed in μmol[CO_2] m^{-2}[leaf] s^{-1} is converted using the constant $10^{-6} \times 30 \times 3600$ into p in g[DM] m^{-2}[leaf] h^{-1}. Photosynthesis per unit ground, $\mathbf{p}$, is obtained from p by multiplying by the sun-lit leaf area index, Λ (in m^2[leaf] m^{-2}[ground]), namely

$$\mathbf{p} = \Lambda p = \Lambda P_{\max} f\{L\} h\{T\} k\{C_a\} \tag{4}$$

Λ itself may be calculated for small plants with all leaves illuminated from a measured value of the structural leaf area ratio, λ, (in m^2[leaf] kg^{-1}[SDM]), and $\mathbf{S}$:

$$\Lambda = \lambda \mathbf{S} \tag{5}$$

where I assume a constant leaf area ratio for seedlings.

Hence, Equation (4) becomes

$$\mathbf{p} = \lambda \mathbf{S} P_{\max} f\{L\} h\{T\} k\{C_a\} \tag{6}$$

I assume that photosynthesis is inhibited in proportion to the NSC available at dawn, as in the steady-state model [9], namely

$$\mathbf{i} = \beta \mathbf{p} \mathbf{C}_d \tag{7}$$

where $\mathbf{C}_d$ is NSC at dawn, and β (m^2[ground] g^{-1}[NSC]) is a positive constant smaller than $1/\mathbf{C}_d$. Consequently, actual photosynthesis, $\mathbf{p} - \mathbf{i}$, is

$$\mathbf{p} - \mathbf{i} = (1 - \beta \mathbf{C}_d) \lambda \mathbf{S} P_{\max} f\{L\} h\{T\} k\{C_a\} \tag{8}$$

Metabolism leading to growth is limited by temperature as well as by NSC. Let $\mathbf{n}\{T\}$ be the maximum rate of metabolism at a given temperature, both conversion to structure and all respiration. I assume this limit increases exponentially with temperature over the entire range

$$\mathbf{n}\{T\} \equiv \mathbf{m}\{T\} + \mathbf{g} + \mathbf{s} = \mathbf{n}_0 \lambda \mathbf{S} \exp\{\zeta T\} \tag{9}$$

where $\mathbf{n}_0$ (in g[DM] m^{-2}[ground] h^{-1}) is metabolism of a crop of size $\lambda\mathbf{S}$ = 1 and at 0 °C.

Maintenance respiration is assumed to increase exponentially, except with a temperature response, θ, that may differ from ζ,

$$\mathbf{m}\{T\} = \mathbf{m}_0 \lambda\mathbf{S} \exp\{\theta T\} \tag{10}$$

Furthermore,

$$\mathbf{n}\{T\} \geq \mathbf{m}\{T\} \tag{11}$$

Structural growth, $\mathbf{s}$, is proportional to growth respiration, $\mathbf{g}$, via the conversion efficiency, $\boldsymbol{\varepsilon}$, from carbon in photosynthate to carbon in structure,

$$\mathbf{s} = \left(\frac{\varepsilon}{1-\varepsilon}\right)\mathbf{g} \tag{12}$$

At high temperature, when $\mathbf{n}\{T\}$ is much greater than $\mathbf{m}\{T\}$, growth is limited by $\boldsymbol{\alpha}$,

$$\mathbf{g} + \mathbf{s} = \frac{1}{1-\varepsilon}\mathbf{g} = \alpha\mathbf{C} \tag{13}$$

Here, $\boldsymbol{\alpha}$, in h^{-1}, the response of growth to NSC, appears to be dependent on photoperiod but independent of temperature. In the light, α_L may have a higher value than in darkness α_D. As long as NSC is not completely depleted, growth continues to utilize NSC.

$$\mathbf{g} + \mathbf{s} = \min\{\alpha\mathbf{C}, \mathbf{n}\{T\} - \mathbf{m}\{T\}\} \tag{14}$$

If NSC is completely depleted while $\mathbf{p} < \mathbf{m}$, maintenance respiration is supported by sacrificing structural material. In that case

$$\mathbf{m} = \mathbf{m}\{T\} \tag{15}$$

To describe the variation in NSC over the diurnal cycle, **S** is normalized to 1 g[SDM] after each iteration. This requires subtracting a term in **Cs**, corresponding to the NSC lost in this renormalization

$$\frac{\mathrm{d}\mathbf{C}}{\mathrm{d}\mathbf{t}} = -C \bullet s \tag{16}$$

Given the states $\mathbf{S}$ and $\mathbf{C}$ of the crop at any point in time, and while $\mathbf{C} > 0$, the terms of Equation (2) may be calculated from Equations (8), (10), and (14),

$$\frac{\mathrm{d}\mathbf{S}}{\mathrm{d}\mathbf{t}} \equiv \mathbf{s} = \varepsilon \ \min\{\boldsymbol{\alpha}\mathbf{C}, \mathbf{n}\{T\} - \mathbf{m}\{T\}\} \tag{17}$$

The rates $\mathbf{p}$ and $\mathbf{m}$ are unaffected by the level of $\mathbf{C}$ in Equation (2). Once the rates $\mathbf{c}$ and $\mathbf{s}$ are known, the next-step values of the states $\mathbf{S}$ and **C** may be calculated, and then the next set of rates and so on.

The parameters for NSC and respiration are expressed in g [CHO] g^{-1}[SDM] h^{-1} (Table 1). The model was simulated in the VENSIM simulation language (Ventana Systems, Harvard, MA, USA), starting with an arbitrary initial state. Five days of periodic weather resulted in a transition to an almost periodic trajectory of **S** and **C**. Relative growth rate on the fifth day, RGR, was calculated from the sum of growth increments over each hour divided by the elapsed time.

Table 1. Parameters used in the dynamic model to simulate growth and non-structural carbohydrate in various crops.

Reference			**[14]**	**[11]**	**[9]**	**[30]**	**[31]**	**[18]**	**[27]**
Parameter	Units	Symbol	Tomato	Bean	Seedling Tomato	Seedling Tomato	Arabidopsis	Melon	Soybean
Maximum photosynthesis	μmol CO_2 m^{-2} s^{-1}	P_{max}			36	45	45	45	45
Half maximum light	μmol[PAR] m^{-2} s^{-1}	γ			309	309	309	309	309
Half maximum CO_2	μmol mol^{-1}	δ			225	225	225	225	225
Temperature optimum for PS	°C	τ			24	24	24	27	27
Decrease per °C from τ	$°C^{-2}$	κ			0.0013	0.0013	0.0013	0.0013	0.0013
PS inhibition factor	g[SDM] g^{-1} [CHO]	β			0.9	1.25	1.25	1.25	1.25
Total respiration at 0 °C	mg[CHO] g^{-1} [SDM] h^{-1}	n_0	0.025	0.05	0.03	0.035	0.035	0.025	0.035
Exponential response of total	$°C^{-1}$	ζ	0.11	0.11	0.11	0.11	0.11	0.11	0.11
Maintenance respiration at 0 °C	mg[CHO] g^{-1} [SDM] h^{-1}	m_0	0.007	0.007	0.007	0.007	0.007	0.007	0.007
Exponential response of maintenance	$°C^{-1}$	θ	0.0693	0.0693	0.0693	0.0693	0.0693	0.0693	0.0693
Conversion efficiency	dmnl	ε	0.75	0.75	0.75	0.75	0.75	0.75	0.75
Growth in dark	h^{-1}	α_D	0.07	0.07	0.07	0.07	0.07	0.07	0.07
Growth in light	h^{-1}	α_L			0.07	0.14	0.14 * 0.28	0.14	0.14

* Values are 0.14 and 0.28 h^{-1} for **COL0** and **pgm**, respectively. The parameters P_{max} and γ are given in units per second and converted to g m^{-2} h^{-1} in the model. Reference refers to the papers with the data simulated here.

3. Parameter Estimation

Altogether, the dynamic model has 14 parameters: P_{max}, γ, κ, τ, δ, λ, β, $\mathbf{n}_0$, ζ, $\mathbf{m}_0$, θ, ε, α_L, and α_D (Table 1). As much as possible, the parameter values used were equivalent to those for tomato in the steady-state model [9]. Values for P_{max}, γ, δ, τ, and κ in Equation (3) were determined by least squares fit to data from measurement of gross photosynthesis of tomato leaves [9], except data were measured at CO_2 concentrations of 200, 400, and 1600 μmol[CO_2] mol^{-1}[air] (data not shown). The regression between measured and observed data was $R^2 = 0.94$. A P_{max} value was found which optimized the prediction of growth rate and NSC over all environments. Leaf area ratio, usually reported per g [DM], was transformed to λ, by subtracting NSC from the actual DM. The parameter β was chosen to optimize the fit between observed and predicted NSC, when it accumulated at cool temperatures. Maintenance respiration, $\mathbf{m}_0$, and its temperature dependence, θ, were determined from observations of dark respiration of tomato leaves at various temperatures [9]. This gave a Q_{10} = 2. The values of parameters describing metabolism, $\mathbf{n}_0$ and ζ, were determined by fitting growth data at temperatures cooler than 20 °C. The resulting Q_{10} = 3, was different from θ for maintenance. A value of 0.75 is used for ε, the parameter related to growth efficiency, based on the analysis of Penning de Vries et al. [32].

The parameter α, the response of growth to NSC, is a new element compared to the steady-state model [9]. Growth and diurnal variation in NSC were sensitive to this parameter at warm temperatures when $\mathbf{n}\{T\}$ did not limit metabolism. A lower limit to α_D was set by the growth rates observed under this condition. An upper limit was set by the minimum NSC content observed, or by the magnitude of the diurnal variation of NSC. The dependence of α_L in the light was given by the losses of NSC over the light period.

4. Results

4.1. Respiration in Prolonged Darkness

Two studies followed respiration in prolonged darkness to understand NSC use without photosynthesis. Respiration in prolonged darkness was simulated for tomato plants (*Solanum lycopersicon*) grown under high or low irradiance before being put in the dark [14]. Plants under different irradiance were of different sizes, and they were converted to values per gram SDM using a multiplier of 500 and 120 g/plant, for plants pre-treated at 1000 and 200 μmol[PAR] m^{-2} s^{-1}, respectively. The simulated dark respiration for plants pre-treated at 1000 μmol[PAR] m^{-2} s^{-1} stayed on a plateau for 15 h before falling exponentially (Figure 2). There was also a small diurnal variation, similar to the light that plants received before being in darkness [14].

The model predicted values similar to those observed until 36 h. Model values were less than observed for the next 12 h. Finally, the model predicted a level of respiration equivalent to maintenance, 0.45 μmol/plant s^{-1} after 57 h, while actual values dropped to 0.2 μmol/plant h^{-1} at 70 or 80 h. One parameter had to be changed relative to the study of tomato seedlings (see the section on temperature and light below). The value $\mathbf{n}_0$ was reduced from 0.035 to 0.025 mg[CHO] g^{-1}[SDM] h^{-1}. This reduced growth respiration compared to seedlings. Plants pre-treated at 200 μmol[PAR] m^{-2} s^{-1} had dark respiration that fell exponentially from 0.5 to 0.06 μmol/plant h^{-1} over 24 h. The model predicted values would fall from 0.39 to 0.15 μmol/plant h^{-1} at 24 h, the value due to maintenance respiration. The correlation between predicted and actual values of respiration was $R^2 = 0.91$ under high light, and $R^2 = 0.61$ under low light, with the $\mathbf{n}_0$ as modified. Respiration rate of bean plants (*Vica faba*) was followed for 14 h in darkness at 15 and 25 °C, after pre-treatment under high or low light [11]. For respiration, I used 1000 * (maintenance + growth respiration), equivalent to mg[CO_2] g^{-1}[SDM] h^{-1}. For high-light plants followed at 25 °C in darkness, dark respiration fell from 7.4 to 3.8 mg[CO_2] g^{-1}[SDM] h^{-1} over 14 h (Figure 3). Using a value of $\mathbf{n}_0 = 0.05$ and an initial NSC of 0.35 g[NSC] g^{-1}[SDM], the dynamic model predicted a similar decrease with time. For high-light plants followed at 15 °C in darkness, dark respiration was at a plateau of 4.7 mg[CO_2] g^{-1}[SDM] h^{-1} for 9 h before

falling to 3.2 mg[CO_2] g^{-1}[SDM] h^{-1}. The model had similar predictions. I had to set the initial NSC at 0.08 g[CHO] g^{-1}[SDM] to get the model predictions under low light. Dark respiration fell from 3.5 to 2.4 mg[CO_2] g^{-1}[SDM] h^{-1} over 14 h for plants at 25 °C. The model predicted a similar trend with time, but offset by 0.5 mg[CO_2] g^{-1}[SDM] h^{-1}. Dark respiration fell from 2.0 to 1.1 mg[CO_2] g^{-1}[SDM] h^{-1} over 14 h for plants at 15 °C in darkness. The model predicted a higher respiration at the beginning of darkness, but values fell to those observed after 14-h. Using the adjusted values for $\mathbf{n_0}$ and initial NSC, the correlation between predicted and actual values ranged from $R^2 = 0.90$ to $R^2 = 0.99$ for all series (Figure 3).

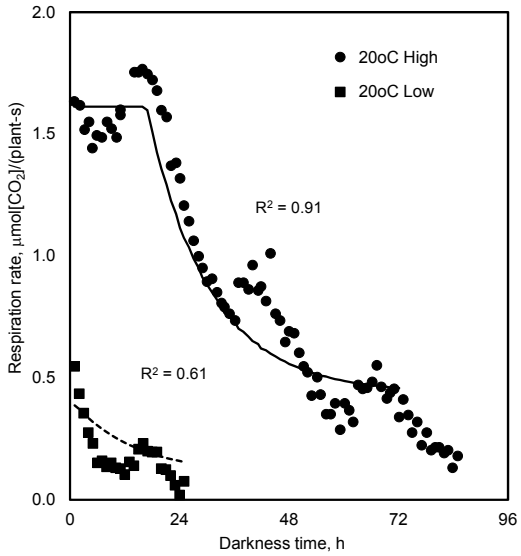

Figure 2. Respiration rate of whole tomato plants in prolonged darkness after pre-treatment under high or low light of 1000 or 200 μmol[PAR]m^{-2} s^{-1} [14]. Filled symbols are measured values for high and low light, and lines are predictions of the dynamic model. The R^2 is given for each time series.

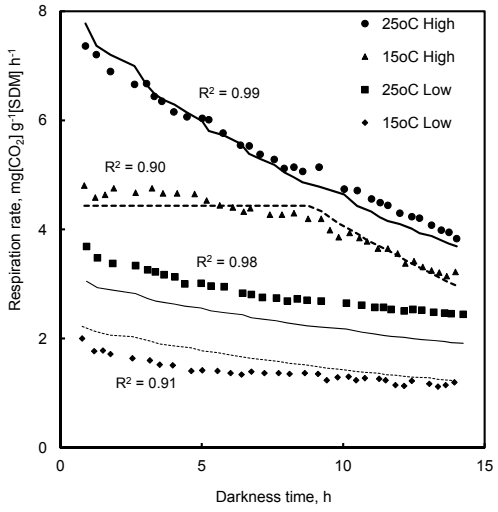

Figure 3. Respiration rate of bean plants in prolonged darkness after pre-treatment under high or low light [11]. Filled symbols are values after pretreatment under high light at 25 and 15 °C, and under low light at 25 at 15 °C, from top to bottom, respectively. Lines are predictions of the dynamic model. The R^2 is given for each time series.

Under high light, for tomato, and for bean at 15 °C, respiration in darkness was first predicted to plateau, when growth respiration was governed by α_D, and then decrease with time, when growth respiration was less than α_D. There was some uncertainty in the prediction of maintenance respiration

in tomato under prolonged darkness. This was not a concern when the model was applied to plants under a normal diurnal cycle, as NSC never fell to zero.

4.2. Effect of Temperature and Light

Relative growth rates and NSC were predicted for tomato seedlings (*Solanum lycopersicon*) grown in a constant environment under various temperatures, and low or high light [30]. Values from the steady-state model [9] were used to estimate parameters for the dynamic model, except that they were converted into hourly rates. There is no "reserve carbohydrate" in the dynamic model. Instead, metabolism was slowed as NSC became depleted, as in Equation (13). Several parameters of the dynamic model were changed with respect to the steady-state model. The maximum photosynthesis rate, P_{max}, was increased from 36, in the steady-state model, to 45 μmol m^{-2} s^{-1}, because a greater fraction of the carbohydrate in the plant was considered when predicting photosynthesis inhibition. The parameter relating NSC to photosynthesis inhibition, $\boldsymbol{\beta}$, was increased from 0.88 to 1.25 g[SDM] g^{-1}[CHO], going from the steady-state to the dynamic model, to more closely predict NSC at low temperatures where it accumulated to a high concentration. In part, this change was likely due to increased photosynthesis, which would otherwise result in greater accumulation of carbohydrate at low temperatures.

The parameters describing rates of respiration and metabolism, such as maintenance respiration, **m**, and the temperature dependence limiting growth demand, **s** in the steady-state model and n here, did not need to be changed in the conversion from a steady-state (Table 1, Column 3) to a dynamic model (Column 4). However, the meaning of the parameter, $\mathbf{n}_0$, changed. It set a limit for growth metabolism alone in the steady-state model, while in the dynamic model, the limit was on the maximum rate at a given temperature of all metabolism, including growth, Equation (9). A value of $\mathbf{n}_0$ = 0.035 mg[CHO] g^{-1}[SDM] h^{-1} in the dynamic model predicted growth rates very similar to the steady-state model (Figure 4), but it also increased NSC (Figure 5). The correlation between predicted and actual values for relative growth rates was similar for the steady-state and the dynamic models, R^2 = 0.74 and R^2 = 0.76, respectively. The single value $\boldsymbol{\alpha}_D$ = 0.07, derived from studies of changes in NSC and respiration for mature tomato plants growing in prolonged darkness [14], was insufficient to describe relative growth rates for the rapidly growing tomato seedlings [30]. When $\boldsymbol{\alpha}$ was constant the model predicted that NSC at the end of the light was higher than observed, while NSC at the end of the dark was lower than observed (data not shown). This was resolved by allowing $\boldsymbol{\alpha}$ to depend on photoperiod. Setting $\boldsymbol{\alpha}_D$ in the dark to one half $\boldsymbol{\alpha}_L$ in the light, $\boldsymbol{\alpha}_D$ = 0.07 h^{-1} and $\boldsymbol{\alpha}_L$ = 0.14 h^{-1}, simulated the diurnal variation in NSC more accurately (Figure 5). In particular, NSC at low temperature was greater for the model than for the data, but the excess NSC was less for the refined than for the initial model. The correlation between predicted and actual minimum values of NSC, was greater for the refined than for the initial dynamic model, R^2 = 0.83 and R^2 = 0.77, respectively. It was much greater that the correlation of minimum values of NSC in the steady-state model, R^2 = 0.65.

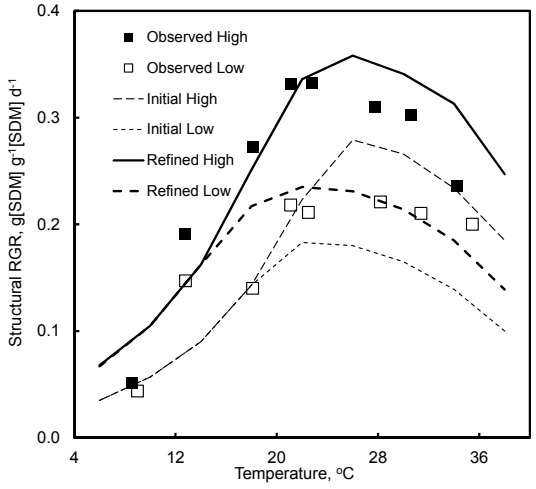

Figure 4. Relative growth rates observed for tomato seedlings over a range of temperatures under low or high light, averaging 110 or 370 μmol[PAR]m^{-2} s^{-1} [30]. Observed values, indicated by symbols, were compared with predictions, lines, from initial and refined versions of the dynamic model.

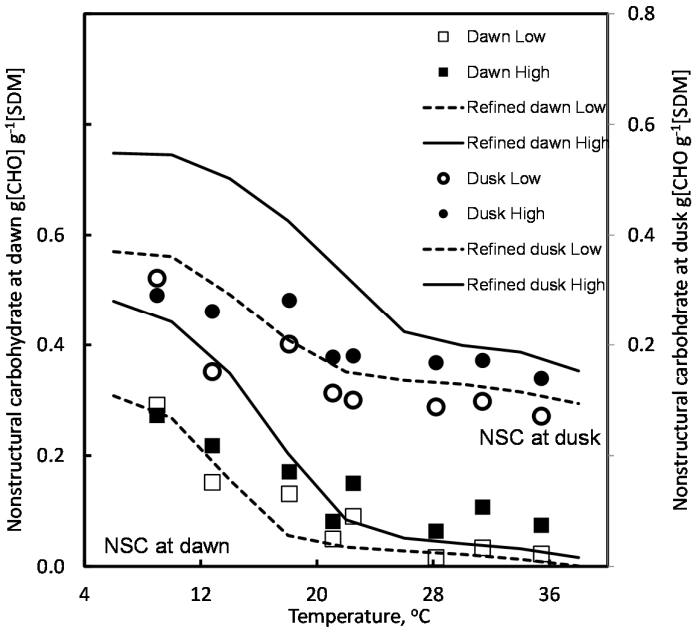

Figure 5. Non-structural carbohydrate at dusk and dawn in tomato seedlings grown over a range of temperatures under low or high light, averaging 110 or 370 μmol[PAR] m^{-2} s^{-1} [30]. Values are offset for dusk and dawn. Symbols represent observed NSC. Predictions are from the dynamic model using parameter values as specified for the refined model, lines.

4.3. Starch and Starch-Less Mutants of Arabidopsis

NSC and growth were predicted for starch synthesizing and starch-less lines, **COL0** and **pgm**, of *Arabidopsis thaliana* [31]. The NSC was observed for various times within a 24-h cycle [31]. A single value of λ = 18.5 m^{-2} kg[SDM] was used as the leaf area ratio to fit the data, along with the photosynthesis parameters for tomato. These parameters gave results in agreement with data, when other model coefficients were the same as the refined values for tomato, except for the starch-less mutant, α_D = 0.28 h^{-1}.

Predictions of NSC at dusk and dawn are given for plants with 6- to 20-h day lengths in Table 2. For starch-synthesizing **COL0**, the dynamic model predicted NSC at dawn would increase up to a 20-h day length. On the other hand, the dynamic model predicted very little NSC in the starch-less mutant, **pgm**, while actual values remained near zero. The values predicted at dusk for **COL0** agreed with measurements, except at a 16-h day length. There was no variation predicted in the starch-less mutant at dusk, whereas the actual values of NSC decreased as photoperiod increased. The decrease in NSC with increased day length was not predicted by either the dynamic or by the steady-state model. The correlation between actual values at dawn, and the values predicted by the dynamic model were R^2 = 0.90 and R^2 = 0.03, for **COL0** and **pgm**, respectively. The minimum NSC from the steady-state model applied to **COL0** had a poorer correlation, R^2 = 0.67. The growth rates were predicted to vary with day length, but they varied little between **COL0** and **pgm** (Table 2). The starch-less mutant was predicted to have faster growth under a longer photoperiod.

Table 2. Effect of photoperiod on non-structural carbohydrate available in starch type, **COL0**, and starch-less, **pgm**, mutants of Arabidopsis. Observations are from Gibon et al. [31] and predictions are from the dynamic model, including relative growth rate. R^2 is the correlation between observed and predicted NSC.

	Non-Structural Carbohydrate				**Relative Growth rate**
	Observed		Predicted		Predicted
Photoperiod	Dawn	Dusk	Dawn	Dusk	
h	g[CHO] g^{-1}[SDM]		g[CHO] g^{-1}[SDM]		g g^{-1} d^{-1}
	Starch type	COL0			
6	0.007	0.046	0.0	0.058	0.048
9	0.009	0.062	0.003	0.069	0.087
12	0.006	0.073	0.011	0.074	0.122
16	0.021	0.095	0.025	0.076	0.166
20	0.051	0.079	0.045	0.075	0.206
R^2			0.90	0.84	
	Starch-less	pgm			
6	0.002	0.058	0.0	0.038	0.047
9	0.002	0.047	0.0	0.041	0.086
12	0.003	0.041	0.001	0.041	0.126
16	0.004	0.024	0.009	0.041	0.175
20	0.002	0.012	0.022	0.040	0.220
R^2			0.03	0.22	

Values of NSC were predicted for **COL0** and **pgm** under a 12-h day length (Figure 6). The dynamic model predicted values at 12-h that were similar to those observed. However, within the photoperiod, the predicted values of NSC were correct for **pgm**, but were underestimated for **COL0** from 2 to 6 h. Both **COL0** and **pgm** had similar levels of NSC at 2 to 6 h, while the model predicted more NSC for **COL0** than **pgm**. The correlation between predicted and actual values was $R^2 = 0.87$ and $R^2 = 0.96$, for **COL0** and **pgm** mutants, respectively.

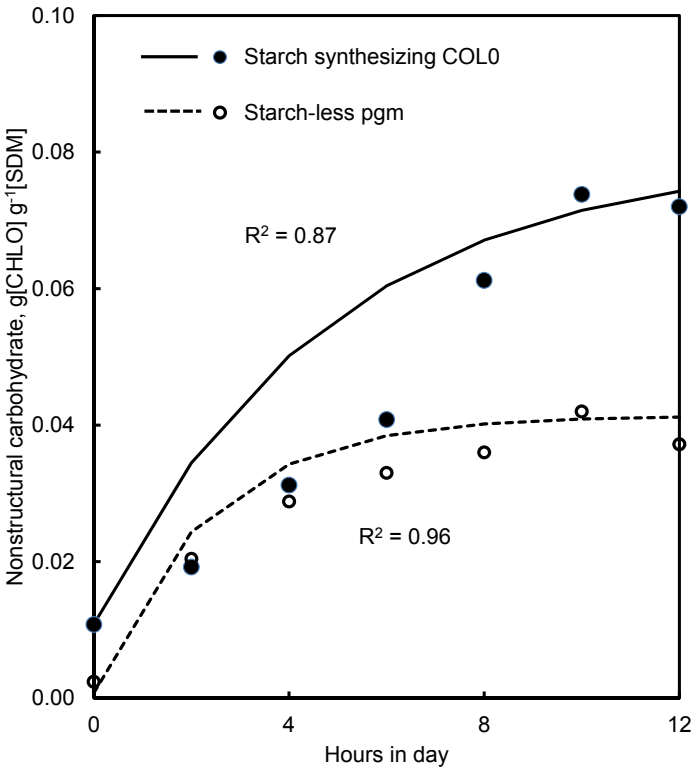

Figure 6. Non-structural carbohydrate in starch synthesizing, **COL0**, or starch-less, **pgm**, mutants of Arabidopsis under a 12-h day length [31] and predictions of the dynamic model. Symbols are data and lines are predictions.

4.4. Effect of CO_2 and Photoperiod

Diurnal variation in NSC was predicted for muskmelon (*Cucumis melo*) grown in a 14 h photoperiod at 20 and 40 °C day temperatures and at 300 and 1500 μmol[CO_2] mol^{-1} [18]. Two parameters had to be altered to more closely fit the data for melon, which was capable of metabolizing NSC to levels much lower than found in tomato seedlings at 20 °C. The relatively large difference in NSC for plants grown at 20 and 40 °C day temperature required $\mathbf{n}_0$ = 0.025 mg[CHO] g^{-1}[SDM] h^{-1}. To better fit the difference in growth at 20 and 40 °C, the optimum temperature for photosynthesis, τ, was raised from 24 to 27 °C. The model with these revised parameters predicted slower growth for melon than tomato at cool temperatures, but faster growth at warm temperatures.

The dynamic model accurately predicted the diurnal variation in NSC within muskmelon plants, as well as the difference between the treatments, and the generally lower NSC in melon compared to tomato. The highest NSC was predicted the end of the light at 20 °C and 1500 μmol[CO_2] mol^{-1} (Figure 7). Presumably, the rate of metabolism at 20 °C was not sufficient to convert this NSC to structural growth. Under 300 μmol[CO_2] mol^{-1}, the NSC was not sufficient for rapid growth at either 20 or 40 °C. The fastest growth at 1500 μmol[CO_2] mol^{-1} was predicted at 40 °C, 0.24 g g^{-1} d^{-1}, compared to 0.21 g g^{-1} d^{-1} at 20 °C. The correlation between predicted and actual values was R^2 = 0.78 to predict NSC and R^2 = 0.84 to predict RGR. The steady-state model could only predict NSC if the reserve carbohydrate had a term for CO_2 concentration, with minimum values of NSC higher at 1500 than 300 μmol[CO_2] mol^{-1}, at both 20 and 40 °C day temperatures.

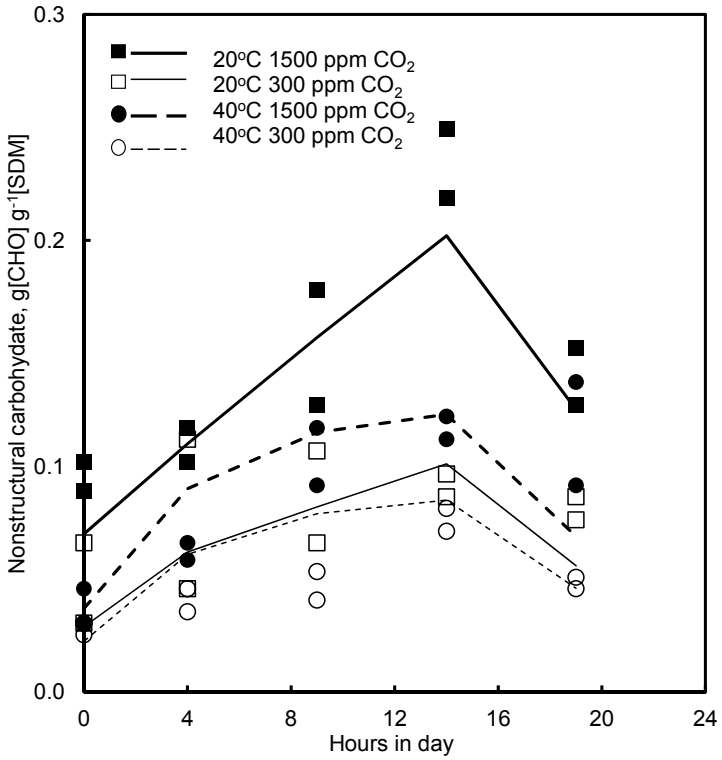

Figure 7. Diurnal variation in NSC observed for melon grown at 20 and 40 °C day temperatures, and at 300 and 1500 μmol[CO_2] mol^{-1} [18]. Symbols are observations from two harvests, at 11 and 22 days of treatment pooled together. Lines are predictions from the dynamic model.

The effect of day length and irradiance on NSC and RGR was predicted for soybean (*Glycine max*) grown under 7- or 14-h day lengths and 320 or 640 μmol[PAR] m^{-2} s^{-1} [27]. The maximum rate of photosynthesis per unit leaf area of soybean occurred under 7-h photoperiod, but the maximum rate per gram SDM occurred under the 14-h photoperiod [27]. Photosynthesis on a per leaf area basis was higher under high light. To account for this in the dynamic model, a higher leaf area ratio was used for plants growing under 7-h than 14-h day length. Values of λ were 32 and 38 m^2 kg^{-1}[SDM] under 7 h photoperiod, and 19 and 24 m^2 kg^{-1}[SDM] under 14-h photoperiod, for 640 and 320 μmol[PAR] m^{-2} s^{-1}, respectively. The optimum temperature for photosynthesis was τ = 27 °C, as for melon. Under a 7-h photoperiod, the NSC values predicted by the dynamic model were similar to those observed (Figure 8). Under a 14-h photoperiod, the values of NSC predicted were more than observed, except at dawn and dusk. Due to changes in λ, the observed and predicted NSC were similar at 320 and 640 μmol[PAR] m^{-2} s^{-1} under the two day lengths. The correlation between predicted and actual NSC values were R^2 = 0.94 and R^2 = 0.72, under 7- and 14-h photoperiods, respectively. The lower NSC seen within the 14-h photoperiod may be a by-product of the experimental methods. The model predicted growth rates of 0.31 vs. 0.26 g g^{-1} d^{-1}, compared to actual net assimilation rates of 0.28 vs. 0.19 g g^{-1} d^{-1}, under 14- compared to 7-h photoperiods at 640 μmol m^{-2} s^{-1}[PAR] [27]. There was little difference due to light intensity.

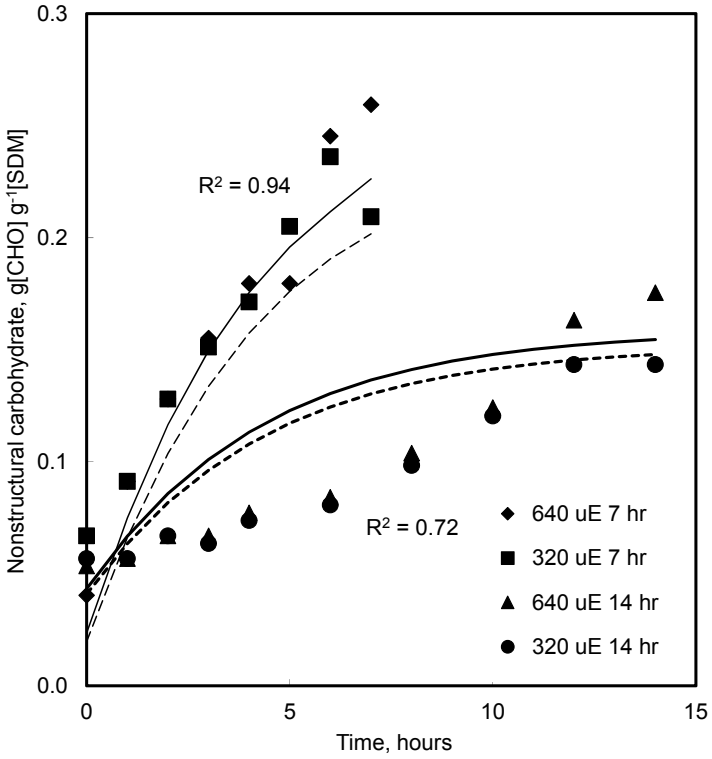

Figure 8. Non-structural carbohydrate content of "Amsoy" soybean grown under 7- or 14-h day lengths and 320 or 640 μmol[PAR] m^{-2} s^{-1} [27]. Symbols are data and lines are predictions of the dynamic model.

5. Discussion

5.1. Temperature Effects on Respiration

This dynamic carbohydrate model of growth was able to metabolize all [CHO], including the "reserve carbohydrate" that was not subject to metabolism in the steady state model. Some features of fitting the model to results for prolonged respiration of tomato in darkness agreed with the reported data and with standard intuition, but some did not. Dark respiration in tomato and bean under both high- and low-light pre-treatment were well fit with an exponential temperature dependence (Figures 2 and 3). The plateau in respiration under high NSC and cool temperature was as expected from Equation (13). The initial substrate in bean was set to 0.35 and 0.08 g[CHO] g^{-1}[SDM], for high- and low-light pre-treatment, respectively. The initial value for high light was slightly greater than that published [14]. The value for low light ensured that respiration had no plateau (Figure 3 lower two curves). Breeze and Elston [11] gave no procedure for measuring TNC, so the values may have changed from one experiment to the next. The values of α_D were the same for tomato and bean.

The temperature dependence of growth respiration, ζ, was greater than that of maintenance, θ, for tomato, and the same values was used for all other species (Table 1). The values were equivalent to $Q_{10} = 3$ for growth and $Q_{10} = 2$ for maintenance. Thus, growth was enhanced by high light at higher temperatures. At sufficiently high temperature, growth was inhibited by photosynthesis and the lack of NSC. Although some scientists think there is a temporal effect of temperature on maintenance respiration, I found a $Q_{10} = 2$ for maintenance of tomato over the range of 10 to 36 °C. It is not clear if the temperature dependence of growth respiration continues to increase above the point where NSC limits growth.

5.2. Dependence of Photosynthesis

About one half of the dynamic model pertains to photosynthesis, the function that supplies NSC for growth. I used non-interacting single-argument functions for light, temperature and CO_2 concentration in Equation (3), all of them non-linear. More complex forms, based on biochemistry of photosynthesis contain interactions between the effects of the environmental factors [8]. Compared to the more complicated function, the form I used gave a sum of squares from regression for tomato of $R^2 = 0.94$, compared to $R^2 = 0.97$ with the Farquhar model. I decided to use the simpler model when predicting photosynthesis for other species.

In the steady-state model, photosynthesis inhibition was determined by the minimum daily NSC. In the dynamic model, photosynthesis inhibition was affected hour by hour, as NSC varied over the day. This had a negative effect on photosynthesis and growth, particularly for young tomato seedlings of [30]. A large fraction of photosynthesis must be inhibited to predict NSC accurately under demand-limited conditions. Relatively little inhibition of photosynthesis is required to predict growth under supply-limited conditions. This combination could be achieved only by relating inhibition to the minimum NSC content over the diurnal cycle, rather than using NSC hour by hour during the day. This agrees with the data of Krapp and Stitt [26] on the increase of starch and photosynthetic inhibition in spinach leaf discs.

5.3. Values for $\mathbf{n}_0$

The parameter related to maximum growth, $\mathbf{n}_0$, varied among the two studies of tomato. The value used to fit the data of Gary et al. [14] was smaller than that used to fit the data for tomato seedlings [30], which were in an earlier stage of growth. Acock et al. [18] found a slower RGR but higher NSC for melon plants that were 10 days older, when grown under the same conditions. This was predicted with a lower value for $\mathbf{n}_0$ for older plants. Other observations in lettuce [33,34] noted that older and larger plants had slower growth but higher NSC than younger and smaller plants. These observations are not reconciled with the dynamic model, which would predict a lower NSC related to self-shading and reduced light intensity per unit leaf area in larger plants. These observations may show that a smaller fraction of total biomass is growing in larger compared to smaller plants.

Another explanation concerns the whole-plant nature of the dynamic model. NSC is found in all plant organs, but in some organs such as stems and tubers, the NSC appears to be in relatively long-term storage, and not immediately used for metabolism. Localized translocation and source-sink relations may affect the distribution of carbohydrate in older plants. The NSC in leaves is usually turned over with a half-life of a few hours, due to metabolism and translocation. (I thank Stephane Adamowicz for this insight.) Young seedlings have a large fraction of biomass in leaves compared to older plants. Thus, a larger fraction of NSC may be metabolically active in young, compared to older, plants. A consequence of this argument is that $\mathbf{n}_0$ should be scaled inversely with plant size to emulate the changing relation between NSC and growth rate. This change in $\mathbf{n}_0$ would correspond to the proportion of actively growing tissue as a fraction of total biomass.

5.4. Starch and Starch-Less Plants

Starch increases in leaves in the day and decreases in the night in a roughly linear fashion [19]. The dynamic model predicted a nonlinear response, with faster use of NSC at dusk and slower use at dawn (Equation (13)). Growth rates may be responding to soluble sugars rather than NSC. The relationship between NSC and growth in the day, $\boldsymbol{\alpha}_L$, was much higher for the starch-less Arabidopsis, **pgm**, than the starch synthesizing, **COL0** [31]. There may be two state storage variables; starch and sugar. The dynamic model using NSC worked well for whole plants, because the NSC in parts other than leaves took a while to equilibrate between sugar and starch, and thus affect respiration and growth in all parts.

5.5. CO_2 and Growth

Carbon dioxide enrichment increased growth of melon but had less effect on NSC. The highest NSC was at 20 °C and 1500 μmol mol^{-1} CO_2 (Figure 7), while the fastest growth was at 40 °C and 1500 μmol[CO_2] mol^{-1} [18]. Plants under 300 μmol[CO_2] mol^{-1} did not have enough NSC for rapid growth at either 20 or 40 °C. Inhibition of photosynthesis is often seen in plants under CO_2 enrichment, especially when CO_2 increases NSC. The high value of NSC under 1500 μmol[CO_2] mol^{-1} resulted in an predicted inhibition of photosynthesis of β = 0.108 and β = 0.044 g[CHO] g^{-1}[SDM] h^{-1}, at 20 °C compared to 40 °C, respectively. The values under 300 μmol[CO_2] mol^{-1} did not differ as much, β = 0.038 and β = 0.024 g[CHO] g^{-1}[SDM] h^{-1}, at 20 and 40 °C. Thus, the dynamic model predicted greater inhibition of photosynthesis under high compared to low CO_2. One value of the dynamic model was that it predicted an inhibition of photosynthesis due to CO_2 enrichment.

5.6. NSC and Growth

The dynamic model retained some NSC at the end of the dark period. This "reserve carbohydrate" was not specified independently of supply and demand, as in the steady-state model [9], where the reserve carbohydrate was not subject to metabolism, and appeared to be related to light intensity or photosynthesis. The dynamic model predicted differences in NSC at dawn, primarily due to differences in light intensity that existed at dusk. The NSC was metabolized at a faster rate in the dark for plants with more NSC at dusk, but it never became equal to that in plants with less NSC. Thus, Equation (16), which limited growth through the dark period, also conserved NSC, even under conditions when the temperature dependence of growth by itself, ($\mathbf{n}\{T\}-\mathbf{m}\{T\}$), predicted all carbohydrate would be consumed.

Some predictions of NSC from the dynamic model were greater than those observed for Arabidopsis plants under a long photoperiod (Table 2 and Figure 5) [31] and for soybean under two day lengths (Figure 8) [27]. However, the dynamic model predicted the correct NSC at the end of the day. I do not know if the errors within the daily cycle were due to the data or due to the model. In any case at any point in the diurnal cycle, NSC in short photoperiod plants should be less than in long photoperiod plants, as long as sugar metabolism is not inhibited early in the day.

6. Summary

A dynamic model of carbohydrate metabolism and growth was tested under various conditions. The dynamic model predicted respiration for plants in extended darkness [11,14]. The dynamic model also better predicted NSC of tomato under two light levels and various temperatures from 9 to 36 °C [30], compared to a steady-state model [9]. Parameters of the dynamic model used to fit tomato also fit data on NSC in starch-synthesizing and starch-less Arabidopsis [31], using NSC as a replacement for sugar or starch. The predictions of the model also fit the CO_2 and temperature response of melon [18], and day length response of soybean [27]. The model was based on data for seedling plants, in which leaf area ratio was specified per unit structural dry matter. Some other parameters would be more important for studies of larger plants, such as the effect of leaf area index on photosynthesis [2,3], and the proportion of the plant that is growing.

7. Experimental Methods

7.1. Respiration in Prolonged Darkness

Two studies followed respiration in prolonged darkness, to understand NSC use without photosynthesis. Ten-week old tomato plants (*Solanum lycopersicon*) were grown under either high or low light conditions, 1000 or 200 μmol[PAR] m^{-2} s^{-1}, before being put in prolonged darkness [14]. At the beginning of darkness, the values of NSC were 0.236 and 0.120 g[CHO] g^{-1}[SDM], under high light and low light, respectively. Another set of values comes from work of Breeze and Elston [11] on bean (*Vicia faba)*. Dark respiration was followed for 14-h in plants that were first adapted to high or low light at 20 °C. These pre-treatments were 200 or 20 W[PAR] m^{-2} (910 and 91 μmol[PAR] m^{-2} s^{-1})

for 18-h light, 6-dark, 18-h light applied to 4–7-week-old plants. The mean NSC after pre-treatment was reported as 0.31 and 0.24 g[CHO] g^{-1}[SDM] under high and low light, respectively.

7.2. Effect of Temperature and Light

Gent [30] examined the response of tomato seedlings "Sonato" to a wide range of temperatures under controlled environment conditions with a 12-h photoperiod. Light and temperature were controlled, and CO_2 concentration was 400–450 μmol[CO_2] mol^{-1}. There were 8 experimental cycles, each at a different temperature, ranging from 9 to 36 °C. Day and night temperatures were the same. Within each experiment, there were two light intensities, averaging 110 and 370 μmol[PAR] m^{-2} s^{-1}. The environment was imposed 5–18 days after germination, first harvest was 2–5 days later, and final harvests were at dusk and dawn, 3–11 days following the first harvest. Total dry mass was determined for all harvests, and leaf area in the final harvest only. The relative growth rate was determined from initial and final harvests. The NSC, equal to starch plus soluble carbohydrate per g[TDM], was determined at dusk and dawn on the final day of the experiment. Observed values were recalculated from Figures 1 and 4 of Gent [30].

7.3. Starch and Starch-Less Mutants of Arabidopsis

Data from Gibon et al. [31] were used to find NSC for various times within a 24 h cycle for *Arabidopsis thaliana* plants with and without starch synthesis. They compared NSC in a wild ecotype, **COL0,** and **pgm,** a line without starch synthesis. The plants were grown in soil as in Thimm et al. [35], under various photoperiods of 140 μmol[PAR] m^{-2} s^{-1} within a 24 h diurnal cycle. I assumed the temperature was 25 °C and CO_2 was 380 μmol[CO_2] mol^{-1}. Vegetative plants were harvested and transferred to liquid nitrogen for analyses. Observed values came from Figures 4–6 of Gibon et al. [31].

7.4. Effect of CO_2 and Photoperiod

A dataset for melon (*Cucumis melo*) "Haogen" [18] was used to compare the effects of temperature and CO_2 concentration on growth. Before treatment, the conditions were 208 μmol[PAR] m^{-2} s^{-1} under a 14-h photoperiod, 30 °C temperature and ambient CO_2. Experimental treatments were applied at 25- or 35-d after sowing. Light and photoperiod were as during the pre-treatment period. Day-time temperatures were 20 or 40 °C, with a common night-time temperature of 20 °C. Plants were grown under either 300 or 1500 μmol[CO_2] mol^{-1} in each temperature regime. Biomass, leaf area, and NSC concentrations were determined in plants harvested 11 d after start of the treatments. Relative growth rates used here are for the younger plants. Specific leaf area was calculated from analysis of temperature and CO_2 concentration effects, and converted to structural leaf area ratio using a constant proportion of 0.6. Observed values were obtained from Figure 2 of Acock et al. [18].

Data of Chatterton and Silvius [27] were used to determine the effect of day length and irradiance on soybean (*Glycine max*) "Amsoy". Young plants were placed in 1.5 L pots filled with vermiculite and grown at an air temperature of 27 °C under irradiance of 320 or 640 μmol[PAR] m^{-2} s^{-1}. The two photoperiods were 7- and 14-h within a 24-h day length. The CO_2 concentration was assumed to be 330 μmol[CO_2] mol^{-1}. Rates of photosynthesis and determination of NSC were from Table 1 and Figure 4 of Chatterton and Silvius [27]. Dry matter was converted to SDM by subtracting NSC per unit DM, and NSC was recalculated from SDM.

The conditions used to simulate all these data are shown in Table 3.

Table 3. Environmental conditions used to simulate growth and non-structural carbohydrate in various crops.

Parameter			[30]	[31]	[18]	[27]
	Units	Symbol	Tomato	Arabidopsis	Melon	Soybean
Light	μmol[PAR] m^{-2} s^{-1}	L	87–134 325–409	140	208	320 640
Temperature	°C	T	9–36	25	20, 40	27
Carbon dioxide concentration	μmol[CO_2] mol^{-1}	C_a	450	380	300 1500	330
Day length	h		12	6–20	14	7, 14
Leaf area ratio	m^2 kg^{-1} [SDM]	λ	32.3–47.9 25.5–38.5	18.5	21, 30 19, 27	18, 20 36, 40

Acknowledgments: I thank Ido Seginer for his contributions to previous manuscripts describing a dynamic carbohydrate supply and demand model of vegetative growth.

Author Contributions: Martin Gent did all the modelling studies described in this manuscript.

Conflicts of Interest: The author declares no conflict of interest.

Abbreviations

Curly brackets, {}, are used exclusively for arguments of functions.

Abbreviations

$\mathbf{C}$	NSC content	g[CHO] m^{-2}[ground], g[CHO] g^{-1}[SDM]
$\mathbf{c}$	Rate of change of $\mathbf{C}$	g[CHO] m^{-2}[ground] h^{-1}, g[CHO] g^{-1}[SDM] h^{-1}
$\mathbf{C_a}$	Carbon dioxide concentration	μmol[CO_2] mol^{-1}[air]
$\mathbf{C_d}$	Minimum NSC content	g[CHO] g^{-1}[SDM]
f	Response of photosynthesis to light	–
$\mathbf{g}$	Growth respiration rate	g[CHO] m^{-2}[ground] h^{-1}, g[CHO] g^{-1}[SDM] h^{-1}
h	Response of photosynthesis to temperature	–
$\mathbf{i}$	Photosynthesis inhibition rate	g[CHO] m^{-2}[ground] h^{-1}, g[CHO] g^{-1}[SDM] h^{-1}
k	Response of photosynthesis to carbon dioxide concentration	–
L	Light flux	μmol[PAR] m^{-2}[leaf] s^{-1}
$\mathbf{m}$	Maintenance respiration rate	g[CHO] m^{-2}[ground] h^{-1}, g[CHO] g^{-1}[SDM] h^{-1}
$\mathbf{m}_0$	Maintenance respiration at 0 °C	g[CHO] m^{-2}[ground] h^{-1}, g[CHO] g^{-1}[SDM] h^{-1}
$\mathbf{n}$	Maximum rate of metabolism	g[CHO] m^{-2}[ground] h^{-1}, g[CHO] g^{-1}[SDM] h^{-1}
$\mathbf{n}_0$	Rate of metabolism at 0 °C	g[CHO] m^{-2}[ground] h^{-1}, g[CHO] g^{-1}[SDM] h^{-1}
P_{max}	Maximum rate of photosynthesis	g[CHO] m^{-2}[leaf] h^{-1}
p	Specific photosynthesis rate	g[CHO] m^{-2}[leaf] h^{-1}
$\mathbf{p}$	Potential gross photosynthesis rate	g[CHO] m^{-2}[ground] h^{-1}, g[CHO] g^{-1}[SDM] h^{-1}
Q_{10}	Temperature quotient: ratio of reaction rates at 10 °C difference	–
$\mathbf{S}$	Structural dry matter content	g[SDM] m^{-2}[ground]
$\mathbf{s}$	Structural growth rate	g[SDM] m^{-2}[ground] h^{-1}, g[SDM] h^{-1}
T	Temperature	°C
t	Time	h
α_D	Response of growth to NSC in the dark	h^{-1}
α_L	Response of growth to NSC in the light	h^{-1}
β	Factor relating photosynthesis inhibition to NSC	g[SDM] g^{-1}[CHO]
γ	Light intensity at half maximum photosynthesis	μmol[PAR] m^{-2}[leaf] s^{-1}

δ	CO_2 concentration at half maximum photosynthesis	μmol[CO_2] mol^{-1}[air]
ε	Growth conversion efficiency	–
ζ	Exponential temperature coefficient for maximum metabolism	$°C^{-1}$
κ	Sensitivity of photosynthesis to temperature	$°C^{-2}$
τ	Threshold temperature for photosynthesis	°C
Λ	Total leaf area index	m^2[leaf] m^{-2}[ground]
λ	Ratio of leaf area to structural dry matter	m^2[leaf] kg^{-1}[SDM]
θ	Exponential temperature coefficient for maintenance respiration	$°C^{-1}$

References

1. Alagarswamy, G.; Boote, K.J.; Allen, L.H.; Jones, J.W. Evaluating the CROPGRO-Soybean model ability to simulate photosynthesis response to carbon dioxide levels. *Agron. J.* **2006**, *98*, 34–42.
2. Kim, S.-H.; Yang, Y.; Timlin, D.L.; Fleischer, D.H.; Dathe, A.; Reddy, R.R.; Staver, K. Modeling temperature responses and biomass in Maize with MAIZSIM. *Agron. J.* **2012**, *104*, 1523–1537.
3. Timlin, D.; Rahman, S.M.L.; Baker, J.; Reddy, V.R.; Fleisher, D.; Quebedeaux, B. Whole plant photosynthesis, development, and carbon partitioning in potato as a function of temperature. *Agron. J.* **2006**, *98*, 1195–1203.
4. Verdoodt, A.; van Ranst, E.; Ye, L. Daily simulation of potential dry matter production of annual field crops in tropical environments. *Agron. J.* **2004**, *96*, 1739–1753.
5. Scaife, M.A. The early relative growth rates of six lettuce cultivars as affected by temperature. *Ann. Appl. Biol.* **1973**, *74*, 119–128.
6. Kemp, D.R.; Blacklow, W.M. Diurnal extension rates of wheat leaves in relation to temperatures and carbohydrate concentrations of the extension zone. *J. Exp. Bot.* **1980**, *31*, 821–828.
7. Yamori, W.; Noguchi, K.; Hikosaka, K.; Terashima, I. Phenotypic plasticity in photosynthetic temperature acclimation among crop species with different cold tolerances. *Plant Physiol.* **2010**, *152*, 388–399.
8. Farquhar, G.D.; von Caemmerer, S.; Berry, J.A. A biochemical model of photosynthetic CO_2 assimilation in leaves of C_3 species. *Planta* **1980**, *149*, 78–90.
9. Gent, M.P.N.; Seginer, I. A carbohydrate supply and demand model of vegetative growth: Response to temperature and light. *Plant Cell Environ.* **2012**, *35*, 1274–1286.
10. Seginer, I.; Gent, M.P.N. Short and long term vegetative growth response to temperature, interpreted by the dynamics of a carbohydrate storage. *Sci. Hort.* **2014**, *171*, 14–26.
11. Breeze, V.; Elston, J. Some effects of temperature and substrate content upon respiration and the carbon balance of field beans (*Vicia faba* L.). *Ann. Bot.* **1978**, *42*, 863–876.
12. Baysdorfer, C.; Warmbrodt, R.D.; VanDerWoude, W.J. Mechanisms of starvation tolerance in pearl millet. *Plant Physiol.* **1988**, *88*, 1381–1385.
13. Brouquisse, R.; Gaudillère, J.P.; Raymond, P. Induction of a carbon-starvation-related proteolysis in whole maize plants submitted to light/dark cycles and to extended darkness. *Plant Physiol.* **1998**, *117*, 1281–1291.
14. Gary, C.; Baldet, P.; Bertin, N.; Devaux, C.; Tchamitchian, M. Time-course of tomato whole-plant respiration and fruit and stem growth during prolonged darkness in relation to carbohydrate reserves. *Ann. Bot.* **2003**, *91*, 1–10.
15. Devaux, C.; Baldet, P.; Joubes, J.; Dieuaide-Noubhani, M.; Just, D.; Chevalier, C.; Raymond, P. Physiological, biochemical and molecular analysis of sugar-starvation responses in tomato roots. *J. Exp. Bot.* **2003**, *54*, 1143–1151.
16. Moser, L.E.; Volenec, J.J.; Nelson, C.J. Respiration, carbohydrate content, and leaf growth of tall fescue. *Crop Sci.* **1982**, *22*, 781–786.
17. Hendershot, K.L.; Volenec, J.J. Shoot growth, dark respiration, and nonstructural carbohydrates of contrasting alfalfa genotypes. *Crop Sci.* **1989**, *29*, 1271–1275.
18. Acock, B.; Acock, M.C.; Pasternak, D. Interactions of CO_2 enrichment and temperature on carbohydrate production and accumulation in muskmelon leaves. *J. Am. Soc. Hort. Sci.* **1990**, *115*, 525–529.

19. Fondy, B.R.; Geiger, D.R.; Servaites, J.C. Photosynthesis, carbohydrate metabolism, and export in *Beta vulgaris* L. and *Phaseolus vulgaris* L. during square and sinusoidal light regimes. *Plant Physiol.* **1989**, *89*, 396–402.
20. Krapp, A.; Stitt, M. An evaluation of direct and indirect mechanisms for the "sink-regulation" of photosynthesis in spinach: Changes in gas exchange, carbohydrates, metabolites, enzyme activities and steady-state transcript levels after cold-girdling source leaves. *Planta* **1995**, *195*, 313–323.
21. Ayari, O.; Dorais, M.; Gosselin, A. Daily variations in photosynthetic efficiency of greenhouse tomato plants during winter and spring. *J. Am. Soc. Hort. Sci.* **2000**, *125*, 235–241.
22. Geiger, D.R.; Servaites, J.C. Diurnal regulation of photosynthetic carbon metabolism in C_3 plants. *Annu. Rev. Plant Biol.* **1994**, *45*, 235–256.
23. Geiger, D.R.; Servaites, J.C.; Fuchs, M.A. Role of starch in carbon translocation and partitioning at the plant level. *Aust. J. Plant Physiol.* **2000**, *27*, 571–582.
24. Gerhardt, R.; Stitt, M.; Heldt, H.W. Subcellular metabolite levels in spinach leaves: Regulation of sucrose synthesis during diurnal alterations in photosynthetic partitioning. *Plant Physiol.* **1987**, *83*, 399–407.
25. Matt, P.; Schurr, U.; Krapp, A.; Stitt, M. Growth of tobacco in short day conditions leads to high starch, low sugars, altered diurnal changes of the Nia transcript and low nitrate reductase activity, and an inhibition of amino acid synthesis. *Planta* **1998**, *207*, 27–41.
26. Zeeman, S.C.; Northrop, F.; Smith, A.M.; Rees, T. A starch-accumulating mutant of *Arabidopsis thaliana* deficient in a chloroplastic starch-hydrolysing enzyme. *Plant J.* **1998**, *153*, 357–365.
27. Chatterton, N.J.; Silvius, J.E. Photosynthate partitioning into starch in soybean leaves: Irradiance level and daily photosynthetic period duration effects. *Plant Physiol.* **1981**, *67*, 257–260.
28. Caspar, T.; Huber, S.C.; Somerville, C.R. Alterations in growth, photosynthesis and respiration in a starch deficient mutant of *Arabidopsis thaliana* (L.) Heynh deficient in chloroplast phosphoglucomutase. *Plant Physiol.* **1985**, *79*, 11–17.
29. Lin, T.P.; Caspar, T.; Somerville, C.R.; Preiss, J. A starch deficient mutant of Arabidopsis thaliana with low ADP glucose pyrophosphorylase activity lacks one of the 2 subunits of the enzyme. *Plant Physiol.* **1988**, *88*, 1175–1181.
30. Gent, M.P.N. Carbohydrate level and growth of tomato plants. II. The effect of irradiance and temperature. *Plant Physiol.* **1986**, *81*, 1075–1079.
31. Gibon, Y.; Blasing, O.E.; Palacios-Rios, N.; Pankovic, D.; Hendriks, J.H.M.; Fisahn, H.; Hohne, M.; Genther, M.; Stitt, M. Adjustment of diurnal starch turnover to short days: Depletion of sugar during the night leads to a temporary inhibition of carbohydrate utilization, accumulation of sugars and post-translational activation of ADP-glucose pyrophosphorylase in the following light period. *Plant J.* **2004**, *39*, 847–862.
32. Penning de Vries, F.W.T.; Witlage, J.M.; Kremer, D. Rates of respiration and structural growth in young wheat, ryegrass, and maize plants in relation to temperature, water stress, and sugar concentration. *Ann. Bot.* **1979**, *44*, 595–609
33. Gent, M.P.N. Composition of hydroponic lettuce: Effect of time of day, plant size, and season. *J. Sci. Food Agric.* **2012**, *92*, 542–550.
34. Van Iersel, M.W. Carbon use efficiency depends on growth respiration, maintenance respiration, and relative growth rate. A case study with lettuce. *Plant Cell Environ.* **2003**, *26*, 1441–1449.
35. Thimm, O.; Blaesing, O.E.; Gibon, Y.; Nagel, A.; Meyer, S.; Krueger, P.; Selbig, J.; Mueller, L.A.; Rhee, S.Y.; Stitt, M. Mapman: A user-driven tool to display genomics data sets onto diagrams of metabolic pathways and other biological processes. *Plant J.* **2004**, *37*, 914–939.